Oil & Gas Science and Technology – Rev. IFP, Vol. 65 (2010), No. 1, pp. 103-113

DOI: 10.2516/ogst/2009026

IFP International Conference
Rencontres Scientifiques de l'IFP

Advances in Hybrid Powertrains
Évolution des motorisations hybrides

Optimal Energy Management in Hybrid Electric Trucks Using Route Information

T. van Keulen[1]*, B. de Jager[1], A. Serrarens[1,2] and M. Steinbuch[1]

1 Control Systems Technology Group, Eindhoven University of Technology, P.O. Box 513, 5600 MB, Eindhoven - The Netherlands
2 Drivetrain Innovations b.v., Croy 46, 5653 LD, Eindhoven - The Netherlands
e-mail: t.a.c.v.keulen@tue.nl - a.g.de.jager@tue.nl - serrarens@dtinnovations.nl - m.steinbuch@tue.nl

* Corresponding author

Résumé — Optimisation de la gestion de l'énergie dans des véhicules poids lourds électriques hybrides utilisant le guidage d'itinéraire – Pour évaluer la Stratégie de Gestion de l'Énergie (SGE) d'un véhicule hybride, on exploite généralement un cycle de conduite donné, souvent certifié. Dans cet article, l'optimisation de l'itinéraire apparaît aussi comme nécessaire. L'optimisation, en particulier, des conditions de freinage du véhicule, par la maximisation de la récupération d'énergie, permet des économies considérables de combustible sur une même distance parcourue. Pour un itinéraire donné (vitesses cibles en fonction de la distance parcourue et de la position), compte tenu des conditions de circulation, des éventuelles données météorologiques et des paramètres de perte du véhicule, on peut estimer les besoins en puissance nécessaire pour le parcourir. Des techniques de Programmation Dynamique (PD) peuvent alors être employées pour prévoir la répartition de puissance optimale pour un parcours donné, sous condition qu'un état de charge cible soit atteint à la fin du parcours. La solution est recalculée périodiquement afin de l'adapter aux nouvelles conditions du parcours (par exemple, aux conditions de circulation) et est utilisée dans une couche plus basse de la SGE en temps réel pour garantir l'état de charge de la batterie ainsi que la consommation d'essence minimale.

Abstract* — *Optimal Energy Management in Hybrid Electric Trucks Using Route Information — *To benchmark a hybrid vehicle's Energy Management Strategy (EMS) usually a given, often certified, velocity trajectory is exploited. In this paper it is reasoned that it is also beneficial to optimize the velocity trajectory. Especially optimizing the vehicle braking trajectories, through maximization of energy recuperation, results in considerable fuel savings on the same traveled distance. Given future route (target velocities as function of traveled distance/location), traffic, and possibly weather information, together with the vehicle's road load parameters, the future power request trajectory can be estimated. Dynamic Programming (DP) techniques can then be used to predict the optimal power split trajectory for the upcoming route, such that a desired state-of-charge at the end of the route is reached. The DP solution is re-calculated at a certain rate in order to adapt to changing conditions, e.g., traffic conditions, and used in a lower level real-time EMS to guarantee both battery state-of-charge as well as minimal fuel consumption.*

INTRODUCTION

A hybrid vehicle employs several power converters instead of one. The main advantage of hybrid electric vehicles is that the vehicle's kinetic and potential energy can be (partially) recovered and stored during braking or driving down hill. The stored energy can be re-used at a later time to provide propelling power to the vehicle. Second advantage of the hybrid structure is that the engine can temporarily generate energy for storage when this is beneficial, or visa versa. The supervisory control algorithm, dealing with the balanced generation and re-use of the stored energy, such that fuel consumption is minimized, is called Energy Management Strategy (EMS).

During the past years, several useful contributions have been made regarding EMS for hybrid vehicles, see, *e.g.*, [1, 2] for an overview. Given prior knowledge of the velocity trajectory, the problem of finding the optimal power split, can be addressed as a problem of minimizing the fuel consumption over a power trajectory as function of time, which turns out to be a nonlinear non convex constrained optimization problem. The objective outlined in this paper is to find a real-time implementable EMS, which has no exact knowledge of the future power trajectory, but, still minimizes fuel consumption. The outcome of this EMS depends upon the requested power trajectory, which is directly related to route and traffic characteristics, vehicle road load parameters, acceleration and deceleration paths.

In several publications it is attempted to adapt the real-time implementable EMS for the current estimate of the future requested power trajectory. The strategies in [3-6] use drive pattern recognition, and make use of characteristic vehicle operating parameters to chose from a set of representative driving patterns and adjust the EMS accordingly. In [7, 8] the special class of problems for vehicles operating in a fixed-route service, where past velocity information of the future route is available, are described. By comparing the current velocity with past information a prediction of the future velocity trajectory can be obtained. With the increasing use of on-board Geographical Information Systems (GIS), [9] proposes to use the future route information to estimate the requested power trajectory. The relation of vehicle mass and road load parameters with the requested power trajectory is not used, however. In [10] it is suggested to estimate the future power trajectory based upon route target velocities, but, fixed values for acceleration and deceleration are used.

All methods discussed above try to optimize the power split for an estimated velocity trajectory, while the authors of this paper concluded in previous work [11] that the decelerations in the route, determining the amount of recoverable energy, have considerable influence on the fuel consumption. This holds especially for commercial vehicles (trucks) because of the large variability of vehicle mass; a truck can be loaded or unloaded changing its mass by a factor 2-3 for distribution trucks.

The main contribution of this paper is to present an EMS, which not only tries to optimize the use of recovered energy, but also to optimize the velocity trajectory on the future route to increase the amount of recoverable energy. This is achieved by modifying the idea of [9, 10], to use future route GIS information. The future power trajectory can be estimated using route (velocity-distance), weather conditions and vehicle information (estimated mass and road load). Using this data, the deceleration paths that obtain maximal recoverable energy in the route can be computed and become available for the driver. This approach is particularly relevant for trucks, as their acceleration-deceleration behavior is fairly predictable [11, 12], while the mass and road load parameters can vary significantly.

Dynamic Programming (DP) is used to calculate, iteratively with relatively slow update rate, an optimal power split trajectory based upon a power request trajectory which is estimated from an on-board navigation system possibly augmented with actual traffic information (congestion, slow traffic, detour, etc.). Besides, the battery state-of-charge can be constrained to reach a desired level at the end of the route. This could be a relevant feature for plug-in hybrid vehicles, or to initiate an electric (emission free) driving mode at a certain point in the route, for example when entering a city shopping area or an indoor distribution center. Information from this predicted optimal power split trajectory is then used in a lower level real-time EMS.

The remainder of this paper is organized as follows: first, the vehicle dynamics are discussed; Section 2 discusses the vehicle mass and road load parameter variations, in Section 3 the construction of a future power trajectory is outlined; Section 4 describes the proposed EMS; in Section 5 a numerical example is presented; finally, we summarize with conclusions and give an outlook of future work.

1 VEHICLE MODEL

In this paper the performance of a medium sized heavy-duty parallel HEV is compared with a conventional truck with the same engine size. The vehicle model takes into account the vehicle longitudinal dynamics, and static nonlinear maps describing the efficiency of combustion engine, electric machine, and battery. The engine and electric machine are situated in front of a six speed automated gearbox and run with the same rotational speed. The gear selection strategy is obtained from the gearbox manufacturer and not further discussed in this paper. Finally, the driver is modeled as a velocity controller, controlling the vehicle velocity towards a set point, using a proportional controller;

$$P_{req}(t) = \max\left(\min\left[K_d(v - v_{target}), P_{max}(\omega)\right], P_{min}\right) \quad (1)$$

Here P_{req} is the power request of the driver, K_d is the proportional feedback gain, v is the vehicle forward velocity, v_{target} is the vehicle target velocity, P_{max} is the maximum available drive power as function of the crankshaft rotational velocity ω, and P_{min} is the maximum available brake power. The combined maximum power of the electric machine and engine is limited to the maximum power of the engine, such that the hybrid vehicle performance corresponds to the conventional vehicle performance. Note this leads to conservative results, since engine downsizing is possible.

The vehicle's road load force is described by;

$$F_{rl}(t) = c_{rol} mg \cos\beta(t) + mg \sin\beta(t) + c_0 + ... \\ + c_1 v(t) + c_{air} \left(v(t) + v_{wind}(t)\right) |v(t) + v_{wind}(t)| \quad (2)$$

In which m is the vehicle mass, v is the vehicle forward velocity, β is the road angle, g is the gravitational constant, c_{rol} is the rolling resistance coefficient, c_0 is the velocity independent drag force, c_1 is the drag coefficient linear related to vehicle velocity. c_0 and c_1 model the drive-line losses as a drag force at the vehicle wheel. c_{air} is the aerodynamic coefficient, and v_{wind} is the wind force. This model only holds for vehicle forward velocities. The longitudinal vehicle dynamics are described by a force balance at the vehicle wheel;

$$m_e \frac{dv(t)}{dt} = F(t) - F_{rl}(t) \quad (3)$$

Here m_e is the effective vehicle inertia including the rotational inertia of the drive-line (a constant value for m_e is used, hereby disregarding inertia fluctuations due to gear setting), F is the resultant drive/brake force of the engine, electric machine, retarder, exhaust brake and/or service brakes.

The prime mover of the truck is a diesel engine, with a maximum power of 136 kW. The engine is modeled as a power converter; see Figure 1, relating the engine output power P_{ICE} to fuel rate $\dot{m}_f$. The different lines show the (nonlinear, non convex) influence of rotational velocity. Besides, for any rotational velocity, the engine is bounded by a maximum torque, see Figure 3.

The hybrid truck has an electric machine as secondary power converter, with a maximum power of 44 kW. The electric machine is also modeled as a power converter, relating the electric power P_b and mechanical power P_{EM}, see Figure 2. The electric machine can work both as a motor and as a generator. At low rotational speeds the electric machine is limited by maximum torque, while at higher rotational speeds the electric machine is limited by maximum power, see Figure 3.

The lithium-ion battery used in the model has a maximum capacity q_{max} of 9 MJ. The state-of-charge $SOC(t)$ is the defined as the electrical charge stored in the battery $q(t)$ divided by the maximum capacity;

$$SOC(t) = \frac{q(t)}{q_{max}} \quad (4)$$

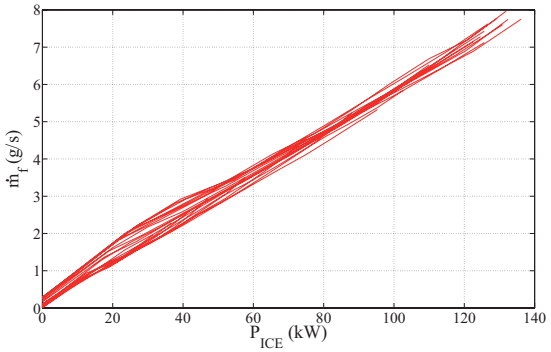

Figure 1

Diesel engine, fuel to mechanical power conversion for different rotational velocities.

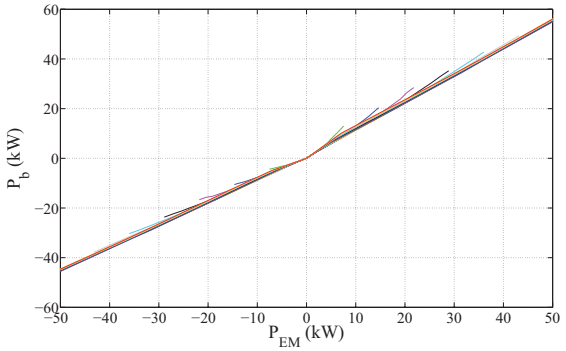

Figure 2

Electric machine, electric P_b to mechanical P_{EM} power conversion for different rotational velocities.

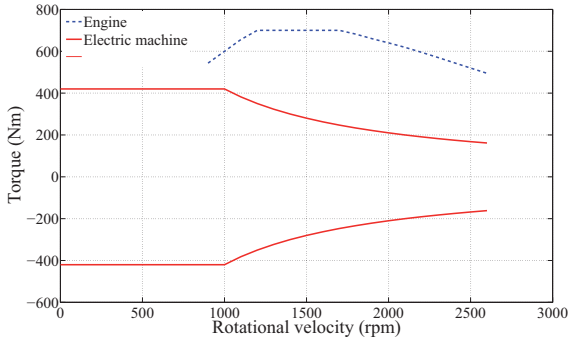

Figure 3

Torque bounds of engine and electric machine as function of rotational velocity.

The battery has losses during charging and discharging. The battery is described with a power based model, see Figure 4. Here P_s is the power that is effectively stored/retrieved

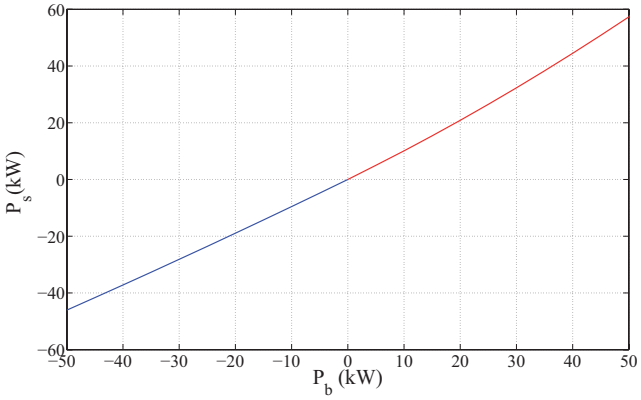

Figure 4

Battery, stored power P_s to electric P_b power conversion.

from the battery, P_b is the electrical power going in/out the electric machine. The losses during charging differ from the losses during discharging. Thermal and transient effects are not considered, nor the influence of state-of-charge.

2 VEHICLE MASS AND ROAD LOAD PARAMETER VARIATION

Our future power trajectory estimation relies on a physical model of the vehicle's longitudinal dynamics. The vehicle dynamics and road load parameters of a heavy-duty vehicle can vary significantly. Obviously, the vehicle mass can vary, by a factor 2-3, due to varying freight; and the road load varies, due to road conditions, ageing and weather conditions such as wind velocity, wind direction, rain and temperature. Therefore, determination of the future power trajectory requires good online estimation of the vehicle mass and road load parameters.

Vehicle mass estimation has been an important research topic, during the last years, in the automation of different vehicle control systems such as anti-lock brake controllers, and gearshift selection in Automated Manual Transmissions (AMTs). Therefore, several contributions can be found concerning the estimation of vehicle mass, see, *e.g.*, [13, 14]. Nevertheless, the simulation model used in this study does not contain a mass estimator, it is assumed the vehicle mass is exactly known. The integration of a mass estimator in the simulation model is part of the future work. In contrary to mass estimation, the estimation of road load parameters has been studied to a lesser extend. For that reason, the parameter variations are discussed below.

The parameter c_{rol} is related to tire rolling losses. The rolling resistance of a tire is a complex function influenced by tire material and construction, thread profile, tire pressure, the vertical load, road surface roughness, rotational velocity, wheel alignment, tire wear and temperature. Experiments show that:

- the rolling resistance increases approximately proportional to the load perpendicular to the road surface [15];
- the rolling resistance has a small increase with increasing rotational velocity [16];
- the rolling resistance decreases with increasing temperature, the sensitivity for temperature influence (heat generation) is strongly related to the thread compound [15]. A higher tire temperature will cause a higher inflation pressure which stiffens the tire; this has a positive effect on the rolling resistance. The rolling resistance of a cold tire compared to a fully warmed up tire can be 15 to 20% higher;
- the rolling resistance decreases with increasing tire pressure [15]. A tire that is inflated towards a pressure of 1 bar below the nominal pressure has a 3% higher rolling resistance;
- the rolling resistance increases with increasing road surface texture. Average rolling resistance differences of 5% can be expected, between steel drum surface and 3M® safety-walk paper, and 30% between smooth steel drum and asphalt [17]. The rolling resistance increases approximately proportional to the road surface mean profile height;
- tire thread profile has considerable influence on the rolling resistance: a truck drive-axle tire has a rolling resistance 5 to 15% higher than a steering-axle tire. Besides, the thread depth has considerable influence upon the rolling resistance: a worn tire with no thread dept has a rolling resistance up to 30% lower than a brand new tire.

Besides, the tires generate rolling resistance due to cornering. On a city route the rolling resistance due to cornering is expected to be significant.

The parameters c_0 and c_1 are related to the drive-line losses, including the losses in suspension, wheel bearings, differential, and gearbox. The total differential and gearbox torque losses are build-up of: gear losses, bearing losses, plunging losses and sealing losses. Experiments show that:

- the best way to model drive-line losses is as a torque loss, rather than an efficiency of power throughput: The losses depend approximately affine on torque and nonlinearly on velocity. Therefore, efficiency as function of power throughput will approach zero for a small absolute value of power;
- the drive-line losses can decrease with 50% due to temperature influences;
- the gearbox losses depend on the selected gear.

The wind velocity and direction v_{wind} can vary significantly (0-30 m/s) and can have considerable influence on the total road load force of heavy-duty vehicles. In this paper

it is assumed that the wind velocity and direction can be obtained from weather information services. The vehicle aerodynamic drag coefficient c_{air} varies for wind velocity and direction, [18] (pp. 7–8) suggests a method to implement the coefficient variation. Besides, c_{air} of heavy-duty vehicles can vary heavily due to different cargo and to air density fluctuations.

In the remainder of this paper it is assumed that both the current vehicle mass, and road load force are perfectly estimated. The discussion above shows that the road load parameters can vary widely, due to different operating conditions. The influence of the parameter variations on the EMS performance will be a topic for future research. Construction of the velocity path, based upon the mass and road load estimation, is discussed in the next section.

3 BUILDING A PREDICTION FOR THE POWER TRAJECTORY USING ROUTE INFORMATION

The real-life driving behavior of trucks during acceleration is to use the full power of the vehicle, even for an unloaded truck [11, 12]. The acceleration rate depends on the power-to-weight ratio of the vehicle. The power-to-weight ratio of trucks shows a large variation due to varying freight weight. Unlike accelerations, the decelerations happen to be driver dependent.

GPS readings in combination with the on-board GIS system, and possibly other sensors as radar or cameras, can be used to obtain route segments of constant road elevation and maximum velocities as function of traveled distance, $\hat{v}_{lim}(x)$. As also outlined by [10] (pp. 77–79) the maximum velocities in the route are determined by velocity limits, maximum cornering velocity or maximum velocities prescribed by traffic, road and/or weather conditions.

At every point at which $\hat{v}_{lim}(x)$ changes to a higher value, full throttle can be applied until the velocity reaches $\hat{v}_{lim}$. Using the vehicle model of Section 1, a velocity trajectory during the accelerations can be constructed $\hat{v}_{acc}(t)$. When $\hat{v}_{lim}(x)$ changes to a lower value, the brake pedal position can be controlled to a required deceleration trajectory. Given the vehicle hybrid system characteristics and road load parameters, a driver independent distance-based deceleration can be constructed that maximizes the recoverable energy on a route, that is the electric machine generates always at its maximum torque/power bound and friction brakes are not used. This is assumed to be optimal because the efficiency of the electric machine is optimal close to its operating bounds. The optimal deceleration rate, at vehicle starting velocity v, is given by;

$$\left.\frac{d\hat{v}(t)}{dt}\right|_{dec}(v, i_{gb}) = \frac{1}{\hat{m}_e}\left(\hat{F}_{rl}(t) + T_{EM\_max}\frac{i_{gb}i_{fd}}{R}\right) \qquad (5)$$

Here, i_{gb} is the current gearbox ratio, i_{fd} is the final drive ratio, R is the wheel radius, $\hat{m}_e$ is the estimated effective vehicle mass, $\hat{F}_{rl}$ is the estimated vehicle road load force described by Equation (2) and $T_{EM\_\max}$ is the maximum torque of the electric machine at the prescribed rotational velocity. The electric machine bounds lead to deceleration rates that are not smooth, and change for different gear ratios. Clearly, a larger electric machine leads to larger optimal deceleration rates. By integrating (5) we obtain the optimal velocity trajectory during braking $\hat{v}_{dec}(t)$. The velocity-distance trajectories $\hat{v}_{acc}(x)$ and $\hat{v}_{dec}(x)$ can easily be calculated from the velocity-time trajectories.

Given a segment starting velocity, a velocity limitation and a velocity at the end of the segment, a velocity trajectory can be constructed, see Figure 5, by computing;

$$\hat{v}_{target}(x) = \min\left(\hat{v}_{lim}(x), \hat{v}_{dec}(x), \hat{v}_{acc}(x)\right) \qquad (6)$$

In Figure 6, it can be seen that an empty truck drives a particular route faster than a loaded truck; optimizing the route for fuel economy, comes with the cost of longer traveling time.

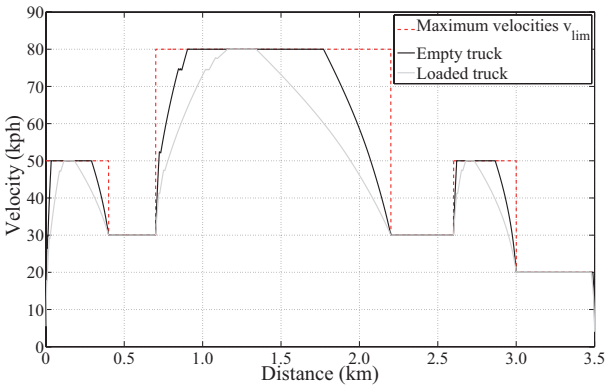

Figure 5

Velocity-distance trajectory with optimal decelerations for both empty and loaded vehicle.

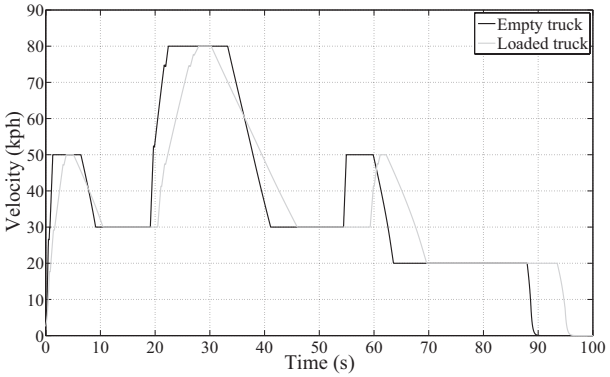

Figure 6

Velocity-time trajectory with optimal decelerations for both empty and loaded vehicle.

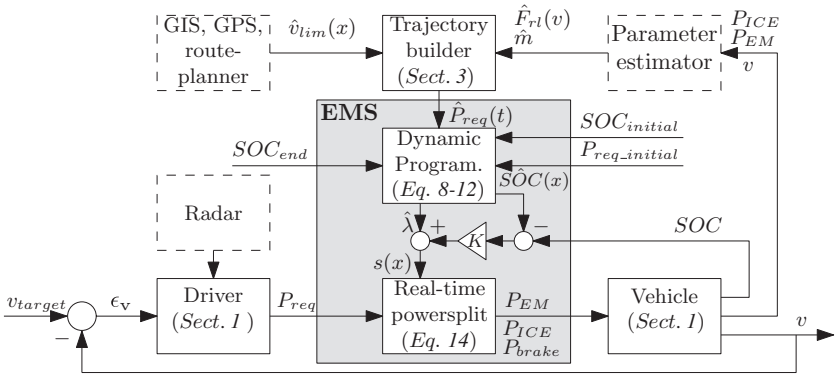

Figure 7

Energy management topology. The blocks Radar, GIS and Parameter estimator are not explicitly explained in this paper and therefore indicated with dashed lines. The block Trajectory-builder is treated in Section 3, the blocks Driver and Vehicle in Section 1. The remaining blocks Dynamic Programming and Real-time EMS form the EMS and are discussed in Section 4. Legend: $\hat{v}_{lim}$ are the predicted maximum velocities in the route, $\hat{m}$ is the estimated vehicle mass, $\hat{F}_{rl}$ is the estimated/predicted road load force, $\hat{P}_{req}(t)$ is the predicted load trajectory, SOC_{end} is the battery state-of-charge at the end of the route, $SOC_{initial}$ is the actual state-of-charge at start of the DP calculation, $P_{req\_initial}$ is the actual power request at the beginning of the DP calculation, $\hat{\lambda}$ is the predicted Lagrange multiplier, $\hat{SOC}(x)$ the predicted state-of-charge trajectory, K is the feedback gain, $s(x)$ the equivalence factor, v_{target} is the actual target velocity, η_v is the velocity error, P_{req} is the actual power request, P_{EM} is the electric machine power, P_{ICE} the engine power, P_{brake} is the service brake power, SOC the actual battery state-of-charge and v the current vehicle velocity.

More comments on the velocity trajectory construction can be found in [19].

The estimated velocity-time trajectory can be used to construct a future power request;

$$\hat{P}_{req}(t) = \hat{F}_{rl}(v)\hat{v}_{target}(t) \tag{7}$$

Here, $\hat{F}_{rl}(v)$ is the predicted road load force where the future velocities, road grade, and wind expectations are incorporated. $\hat{P}_{req}(t)$ can be used as input for a DP algorithm to estimate the optimal power split trajectory.

4 OUTLINE ENERGY MANAGEMENT STRATEGY

We propose to use a hierarchical control structure, see Figure 7. The control structure consist of a trajectory-builder block which receives future maximum velocities $\hat{v}_{lim}(x)$ from the GIS, GPS readings, as well as a mass $\hat{m}$ and road load $\hat{F}_{rl}(v)$ estimation. Based upon these signals the trajectory-builder predicts a future power trajectory $\hat{P}_{req}(t)$ using assumptions on acceleration and deceleration behavior, as was outlined in previous sections.

The predicted power trajectory $\hat{P}_{req}(t)$ is input to a DP algorithm. Given $\hat{P}_{req}(t)$, the current battery state-of-charge $SOC_{initial}$, and current power request $P_{req\_initial}$, the DP algorithm computes the optimal power split trajectory, between the internal combustion engine power P_{ICE}, and the electric machine power P_{EM}, as function of the upcoming route. Hereby fulfilling the equation;

$$\hat{P}_{req}(t) = \hat{P}_{EM}(t) + \hat{P}_{ICE}(t) \tag{8}$$

To guarantee a charge sustainable solution we require a battery state-of-charge at the end of the route or at an intermediate point (but end of horizon) equal to SOC_{end}. Static maps of internal combustion engine, electric machine and battery, as shown in Section 1, are included in the algorithm.

As stated before, the EMS problem of a hybrid vehicle can be formulated as a nonlinear non convex constrained optimization problem over the route, using P_{EM} as the control variable, subject to a battery end-point constraint and several power constraints on the components;

$$\min_{\hat{P}_{EM}(t)} \int_0^{t_f} \dot{m}_{fuel}(P_{EM}, t)dt, \tag{9}$$

s.t.:

$$\int_0^{t_f} P_s(P_{EM}, t)dt = q_{max}\,(SOC_{end} - SOC_{initial}) \tag{10a}$$

$$P_{EM\_min} \le P_{EM} \le P_{EM\_max} \tag{10b}$$

$$P_{ICE\_min} \le P_{ICE} \le P_{ICE\_max} \tag{10c}$$

$$P_{b\_min} \le P_b \le P_{b\_max} \tag{10d}$$

$$T_{EM\_min} \le T_{EM} \le T_{EM\_max} \tag{10e}$$

$$T_{ICE\_min} \le T_{ICE} \le T_{ICE\_max} \tag{10f}$$

$$SOC_{min} \le SOC \le SOC_{max} \tag{10g}$$

Equation (9) and (10a) be solved with DP techniques, the solution of this problem can be found in literature [2,20,21]. The DP algorithm requires a high computational effort. Therefore, the DP calculation is done iteratively, in order to

update the estimated power split trajectory to changing conditions as the vehicle is driving along the route. Equation (9) can be rewritten, using the method of Lagrange multipliers. In literature this is often referred to as Equivalent Consumption Minimization Strategies (ECMS). The optimal power split can be found solving;

$$\min_{\hat{P}_{EM}(t),\hat{\lambda}} \left(\dot{m}_{fuel}(P_{EM,t}) + \hat{\lambda} P_s(P_{EM})\right), \tag{11}$$

subject to Equation (10b-g). The optimization over a trajectory reduces to an optimization only depending on current data; all future trajectory dependency is lumped into the Lagrange multiplier $\hat{\lambda}$, which is obtained from the DP calculation by;

$$\hat{\lambda} = \frac{\partial \dot{m}_{fuel}(P_{EM}, t)}{\partial P_s} \tag{12}$$

Besides, the DP algorithm generates an electric machine power trajectory prediction as function of time, which can be recalculated to a battery state-of-charge trajectory as function of distance: $S\hat{O}C(x)$.

However, due to wrongly predicted target velocities or poorly estimated road load parameters, $\hat{\lambda}$ could deviate from the optimal value. In order to prevent the battery from over/under charging, $\hat{\lambda}$ can be substituted, in real-time, by an estimated equivalence factor $s(x)$. Feedback on the battery state-of-charge is proposed to estimate $s(x)$. This technique was also used in [20, 21].

$$s(x) = \hat{\lambda} + K\left(S\hat{O}C(x) - SOC(x)\right) \tag{13}$$

Here, K is the feedback gain.

The current operating conditions (traffic, weather, route, etc.) dictate a target velocity v_{target}. The driver (or driver aid as adaptive cruise control) operates as a velocity controller, controlling the vehicle velocity towards the target velocity. Output of the driver is a power request P_{req}, see Equation (1), which in practice deviates from $\hat{P}_{req}$. Given P_{req} and $s(x)$ the power split can be determined in real-time by the minimization;

$$\min_{P_{EM}} \left(\dot{m}_{fuel}(P_{EM}) + s(x) P_s(P_{EM})\right) \tag{14}$$

Given the value of $s(x)$, this is a minimization problem that requires virtually no computational effort.

5 SIMULATION EXAMPLE

The purpose of this simulation example is to show the benefit of vehicle mass and route information, and the necessity of updating for sustainable battery charging. This approach is implemented on one of the routes proposed in the SAE recommended practice for measuring fuel economy and emissions of hybrid-electric and conventional heavy-duty vehicles [22]: the higher-speed operation heavy-duty Urban Dynamometer Driving Schedule (UDDS), see Figure 8 for the velocity-distance trajectory. Two vehicle masses are simulated; an empty truck and a fully loaded truck.

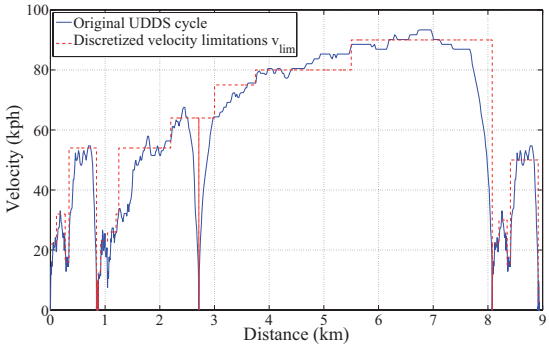

Figure 8

Heavy-duty Urban Dynamometer Driving Schedule (UDDS) velocity-distance trajectory, and the discretized velocity trajectory.

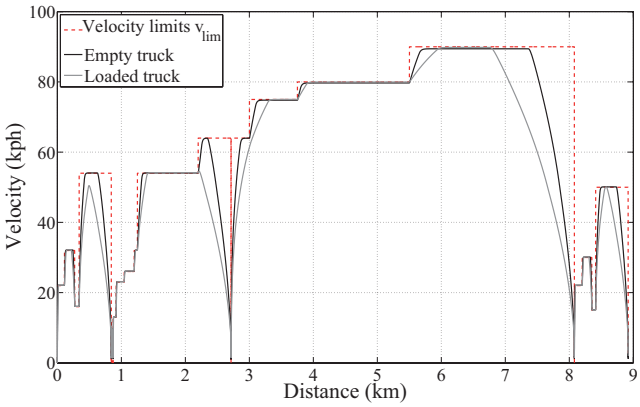

Figure 9

Discretized UDDS cycle with optimal velocity trajectories ($\hat{v}_{target}$) for both empty and loaded truck.

Figure 9 shows the discretized target velocities in the UDDS cycle and the predicted velocity trajectory, using optimal decelerations. Figure 10 shows the same route, however, now it is assumed that we receive information, at point A in the route (at a distance 2.7 km from the start), of traffic congestion later on in the route. Congestion is modeled, arbitrarily, as a lower target velocity and some stops.

The velocity-distance trajectory, together with the predicted road load trajectory is assumed to be perfectly known in this simulation example, and is used as DP algorithm input. Simulation parameters are depicted in Table 1.

The output of the DP algorithm is the predicted state-of-charge profile $S\hat{O}C(x)$, for the original UDDS cycle, see Figure 11; and the UDDS cycle with optimal decelerations,

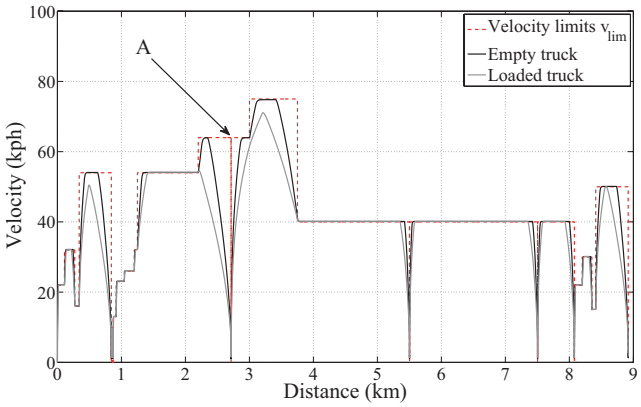

Figure 10

Congested UDDS cycle with optimal velocity trajectories ($\hat{v}_{target}$) for both empty and loaded truck.

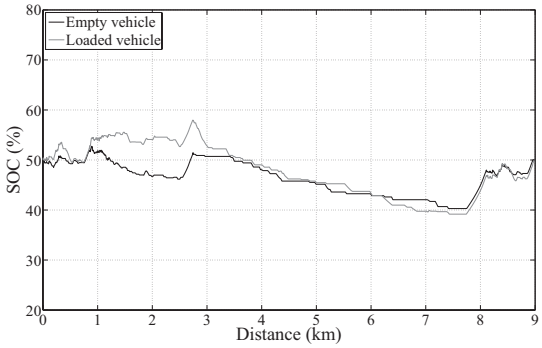

Figure 11

Dynamic programming results of the battery state-of-charge trajectory on the original UDDS cycle for both empty and loaded vehicle.

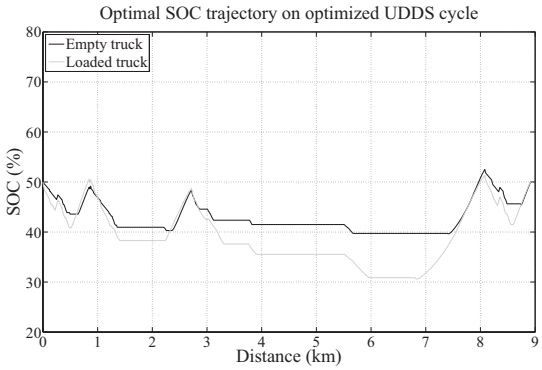

Figure 12

Dynamic programming results of the battery state-of-charge trajectory on the UDDS cycle with optimal deceleration trajectories for both empty and loaded vehicle.

see Figure 12. Comparing Figure 11 and 12, it can be seen that during the decelerations, significantly more energy is recuperated and stored in the battery. Moreover, the increased kinetic energy of the loaded truck, compared to the empty truck, is exploited in the optimized route. This can also be seen in the results presented in Table 2, comparing the fuel consumption of the *empty* conventional and hybrid truck on the original route 1a, and optimized route 1b, with the fuel consumption of the *loaded* conventional and hybrid truck on the original 2a and optimized route 2b. The loaded truck fuel savings in terms of percentage are significantly larger then of the empty truck. Furthermore, both the hybridization of the drive line and use of the route optimization, leads to a fuel saving of 19.0% for an empty truck, and 33.7% for a loaded truck.

In case of the congested route, a new DP calculation is performed, from point A on, using the battery state-of-charge at that particular moment as the new initial value. See Figure 13 for the empty vehicle results and Figure 14 for the results of the loaded vehicle. The new calculated optimal state-of-charge trajectory, from point A on, is shown by the grey solid line. The black line indicates the global optimal solution, calculated if the congestion was known from the start.

It can be seen that the optimal state-of-charge trajectory on the congested route deviates from the initial optimal state-of-charge trajectory. Clearly, the original solution is a suboptimal solution since it deviates from the black line. The dashed line shows the state-of-charge trajectory obtained by using the initial value of $\hat{\lambda}$; that is the $\hat{\lambda}$ calculated over the initial route.

The DP results of the empty vehicle see Figure 13, suggest that it is beneficial to deplete the battery during the first part of the congestion and recharge the battery during the second part of the congestion. We remark that this might

TABLE 1

Simulation parameters corresponding to Equations (1-3) and (19)

Parameter	Description	Value
c_{rol}	Rolling resis.	0.0075 (-)
c_0	loss par.	35 (N)
c_1	vel. loss par.	0.9 (Ns/m)
c_{air}	Aerodyn. loss	3.5 (Ns^2/m^2)
m	Empty mass	9000 (kg)
	Loaded mass	18 000 (kg)
m_e	Eff. veh. mass	m+350 (kg)
β	Road angle	0 (rad)
v_{wind}	Wind velocity	0 (m/s)
K_d	Driver fb gain	300 000 (-)
K	SOC fb gain	0 (-)

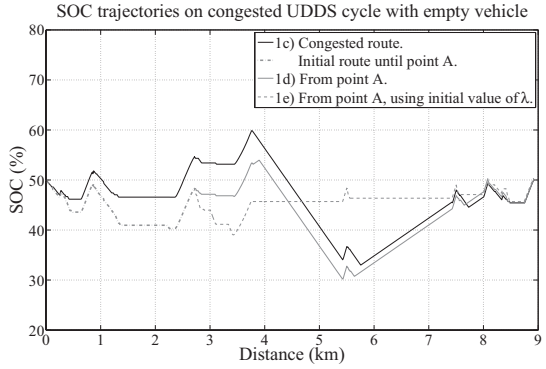

Figure 13

Dynamic programming results of the battery state-of-charge trajectory on the congested UDDS cycle with an empty vehicle.

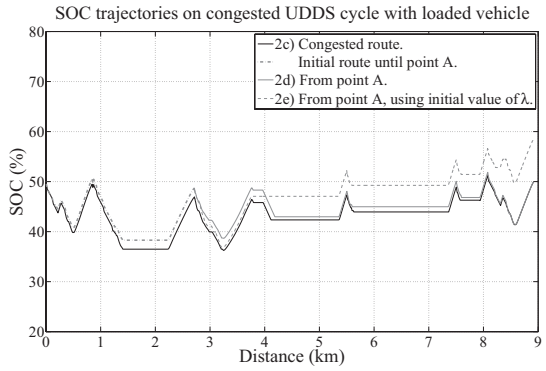

Figure 14

Dynamic programming results of the battery state-of-charge trajectory on the congested UDDS cycle with a loaded vehicle.

be induced by numerical issues during interpolation, rather than on real physical grounds. In future work we will reconsider the use of an engine map as engine model. Especially the non convex character of the measured map is bothersome.

The state-of-charge trajectory obtained using the initial value of $\hat{\lambda}$, shows a different behavior; it remains constant during the congestion parts. Nevertheless, the fuel consumption obtained deviates only marginally from the DP results, see Table 2. From a battery life-time point of view this result could be considered an improvement.

In Figure 14, the battery state-of-charge trajectory using the initial value of $\hat{\lambda}$ shows a similar trajectory as the DP results. However, the state-of-charge end-point deviates. The difference in fuel consumption is again marginal. We conclude that updating the route is useful in retaining the battery state-of-charge within the boundaries, and is less useful to obtain optimal fuel consumption.

Table 2 shows the fuel consumption results for the different simulations. First the empty vehicle results are shown 1), secondly the loaded vehicle results 2). The second column provides the fuel consumption, for the conventional vehicle on the different velocity trajectories. The third column shows the fuel consumption, as well as the relative improvement, of the hybrid vehicle for five different situations:

- the global optimal savings on the original UDDS route;
- the global optimum calculated with DP for the initial route with optimal braking trajectories;
- the global optimum calculated with DP for the congested route;
- the new calculated optimum onwards from point A in the route, see Figure 10, and the solid line in Figure 13, and finally;
- the result obtained when no adjustment is made and the initial calculated $\hat{\lambda}$ is used.

The latter result obviously gives a difference in battery state-of-charge, and therefore, the fuel consumption value is corrected for this difference. The global optimum from point A onwards deviates from the total global optimum, the solution is suboptimal as the optimum battery state-of-charge could not anticipate for the congested part of the route before point A. Because of lower average vehicle speed, the congested route is overall more fuel efficient than the initial route.

CONCLUSIONS AND OUTLOOK

The largest benefit of predictive information is that optimal deceleration paths, that maximize the recoverable energy,

TABLE 2

Simulation results on: a) the original UDDS cycle with DP, b) the optimized UDDS cycle with DP, c) b + congestion with DP, d) b + congestion with $s(x)$ using $K = 0$, e) b + congestion with $\hat{\lambda}$ determined on b

Route	Conventional (g)	Hybrid (g)
Empty truck		
1a	1493	1386 (-7.2%)
1b	1352	1210 (-10.5%)
1c	1077	941 (-12.6%)
1d	1077	948 (-12.0%)
1e	1077	966 -2%ΔSOC
		958 (-11.0%)
Loaded truck		
2a	2285	2099 (-8.1%)
2b	1772	1514 (-14.6%)
2c	1529	1266 (-17.2%)
2d	1529	1270 (-16.9%)
2e	1529	1309-8%ΔSOC
		1276 (-16.5%)

can be incorporated in the route. The second benefit is that the battery's state-of-charge can remain within the operating bounds and can achieve a desired state-of-charge at the end of the route.

The use of GPS or GIS, providing future route information, together with road load force estimation, in the calculation of the optimal EMS, enables adaption of the EMS both for route changes, as well as for vehicle parameters variations. Distance-based trajectories are preferable, since they allow for optimization of the power requested based upon GIS map data, without changing maximum and minimum route vehicle velocities as well as the exact location of full vehicle stops.

Heavy-duty vehicle operation is widely influenced by vehicle parameter variations and changing environmental conditions, making a good prediction of the future power trajectory difficult, on the other hand there are an increasing number of sensors that accommodate estimation of these parameters and conditions. Further research should determine the level of accuracy required from GIS and parameter estimation schemes in order to obtain a power trajectory that is useful for fuel consumption minimization. Topic of research is also the fusion of information from the different sensors and information systems, such as radar, GPS, GIS, vision, CANbus, etc. Besides, we will investigate the possibilities of incorporating elevation, weather and traffic light information, including duration of stops, into the prediction.

The discretization of GIS data, as well as the use of this information, by driver aids as adaptive cruise control is a topic of current research. First results are presented in [19]. Moreover, the results presented in this paper indicate that the optimized route enables significant fuel savings, however, with a cost in travel time. Future work will focuss on route optimization subject to a time constraint. Allowing the driver to make a balanced choice between fuel savings and travel time.

ACKNOWLEDGEMENTS

The research presented in this paper is part of a more extensive project in the development of advanced energy management control for urban distribution trucks which has been made possible by TNO Business Unit Automotive in cooperation with DAF Trucks NV.

REFERENCES

1 Pisu P., Rizzoni G. (2007) A Comparative Study Of Supervisory Control Strategies for Hybrid Electric Vehicles, *IEEE T. Contr. Syst. T.* **15**, 3, 506-518.

2 Sciarretta A., Guzzella L. (2007) Control of Hybrid Electric Vehicles, *IEEE Contr. Syst. Mag.* **27**, 2, 60-70.

3 Jeon S., Jo S., Park Y., Lee J. (1987) Multi-Mode Driving Control of a Parallel Hybrid Electric Vehicle Using Driving Pattern Recognition, *J. Dyn. Syst.- T. ASME* **124**, 141-149.

4 Lin C.C., Jeon S., Peng H., Lee J.M. (2004) Driving Pattern Recognition for Control of Hybrid Electric Trucks, *Vehicle Syst. Dyn.* **42**, 1-2, 41-58.

5 Musardo C., Rizzoni G. (2005) A-ECMS An Adaptive Algorithm for Hybrid Electric Vehicle Energy Management, *IEEE Conference on Decision and Control, and the European Control Conference 2005*, Seville, Spain, December 12-15, 2005, pp. 1816-1823.

6 Yokoi Y., Ichikawa S., Doki S., Okuma S., Naitou T., Shiimado T., Miki N. (2004) Driving Pattern Prediction for an Energy Management System of Hybrid Electric Vehicles in a Specific Driving Course, *The 30th Annual Conf. of the IEEE Industrial Electronics Society*, Busan, Korea, November 2-6, 2004, pp. 1727-1732.

7 Bartholomaeus R., Klingner M., Lehnert M. (2008) Prediction of power demand for hybrid vehicles operating in fixed-route service, *Proceedings of the 17th IFAC World Congress*, Seoul, Korea, July 6-11, 2008, pp. 5640-5645.

8 Kermani S., Delprat S., Guerra T.M., Trigui R. (2008) Real Time Control of Hybrid Electric Vehicle on a Prescribed Route, *Proceedings of the 17th IFAC World Congress*, Seoul, Korea, July 6-11, 2008, pp. 3354-3361.

9 Gong Q., Li Y., Peng Z. (2007) Optimal Power Management of Plug-in HEV with Intelligent Transportation System, *IEEE/ASME International Conference on Advanced Intelligent Mechatronics*, Vol. 4, No. 7, pp. 1-6, September 2007.

10 Back M. (2005) Prädiktive Antriebsregelung zum energie optimalen Betrieb von Hybridfahrzeugen, *PhD Thesis*, available: www.ubka.uni-karlsruhe.de, Univ. Karlsruhe.

11 Keulen van T., Jager de B., Steinbuch M. (2008) Influence of Driver, Route and Vehicle Mass on Hybrid Electric Truck Fuel Economy, *AVEC '08 9th International Symposium on Advanced Vehicle Control*, Kobe, Japan, October 6-9, 2008, pp. 911-916.

12 Bruneel H. (2000) Heavy Duty Testing Cycles Development: A New Methology, *International Spring Fuels & Lubricants Meeting & Exposition*, Paris, France, June 19-20, 2000, SAE 2000-01-1890.

13 Kolmanovsky I., Winstead V. (2006) A Receding Horizon Optimal Control Approach to Active State and Parameter Estimation in Automotive Systems, *Proceedings of the 2006 IEEE International Conference on Control Applications*, Munich, Germany, October 4-6, 2006, pp. 2796-2801.

14 Vahidi A., Stefanopoulou A., Peng H. (2005) Recursive least squares with forgetting for online estimation of vehicle mass and road grade: theory and experiments, *Vehicle Syst. Dyn.* **43**, 1, 31-55.

15 Luchini J.R., Peters J.M., Arthur R.H. (1994) Tire Rolling Computation with the Final Element Method, *Tire Science and Technology*, TSTCA, Vol. 22, No. 4, pp. 206-222, October-December 1994.

16 Stutts D.S., Soedel W. (1992) A Simplified Dynamic Model of the Effect of Internal Damping on the Rolling Resistance in Pneumatic Tires, *J. Sound Vib.* **155**, 1, 153-164.

17 deRaad L.W. (1978) The Influence of Road Surface Texture on Tire Rolling Resistance, *SAE paper* 780257, 1978.

18 Society of Automotive Engineers (1996) J1263 Road Load Measurement and Dynamometer Simulation Using Coastdown Techniques, *SAE Standard*.

19 Keulen van T., Naus G., Jager de B., Molengraft van de R., Steinbuch M., Aneke E. (2009) Predictive Cruise Control in Hybrid Electric Vehicles, *The 24th International Battery, Hybrid and Fuel Cell Electric Vehicle Symposium, EVS24*, Stavanger, Norway, May 13-16, 2009 (accepted).

20 Keulen van T., Jager de B., Steinbuch M. (2008) An Adaptive Sub-Optimal Energy Management Strategy for Hybrid Drivetrains, *Proceedings of the 17th IFAC World Congress*, Seoul, Korea, July 6-11, 2008, pp. 102-107.

21 Koot M., Kessels J., Jager de B., Heemels W., Bosch van den P., Steinbuch M. (2005) Energy Management Strategies for Vehicular Electric Power Systems, *IEEE T. Veh. Technol.* **54**, 3, 771-782.

22 Society of Automotive Engineers (2002) J2711 Recommended Practice for Measuring Fuel Economy and Emissions of Hybrid- Electric and Conventional Heavy-Duty Vehicles, *SAE Standard*.

Final manuscript received in April 2009
Published online in August 2009